TURBULENT FLOW OF LIQUID STEEL AND ARGON BUBBLES IN SLIDE-GATE TUNDISH NOZZLES PART II: EFFECT OF OPERATION CONDITIONS AND NOZZLE DESIGN

Hua Bai and Brian G. Thomas

Hua Bai, Senior research engineer, is with the Dow Chemical Company, 2301 N. Brazosport Blvd., Freeport, TX 77541, and Brian G. Thomas, Professor, is with the Department of Mechanical and Industrial Engineering, University of Illinois at Urbana-Champaign, 1206 W. Green Street, Urbana, IL 61801

ABSTRACT

A three-dimensional finite difference model, developed and validated in Part I of this two-part paper, is employed to study steady-state two-phase turbulent flow of liquid steel and argon bubbles through slide-gate tundish nozzles. Parametric studies are performed to investigate the effects of gas injection, slide-gate orientation, casting speed, gate opening, bubble size, port angle and port shape on the flow pattern and characteristics of the jet exiting the nozzle port. Argon gas injection bends the jet angle upward, enhances the turbulence level, and reduces the size of the back flow zone. Gas injection becomes less influential with increasing casting speed. The off-center blocking effect of the slide-gate generates asymmetric flow that changes with the gate orientation. The 0° gate orientation creates the worst biased flow between the two ports. The 90° orientation generates significant swirl and directs the jet slightly toward one of the wide faces. The 45° orientation generates both types of asymmetry, so appears undesirable. The horizontal jet angle indicates asymmetric flow in the horizontal plane. It increases with decreasing gate opening and decreasing gas injection, and ranges from 3°-5°. Most jet characteristics reach their maximum or minimum values near the critical opening of 60% (linear). Larger bubbles exert a greater influence on the flow pattern. The vertical jet angle becomes steeper with steeper port angle and more slender

port shape. These results will be useful for nozzle design and for future modeling of flow in the mold.

KEY WORDS: Multiphase flow, Turbulence, Numerical model, Continuous Casting, Argon injection, Slide-gate nozzle, Jet characteristics, Port design

I. INTRODUCTION

The tundish nozzle has an important influence on steel quality through its effect on the flow pattern in the mold since the nozzle governs the speed, direction and other characteristics of the jet entering the mold. There is great incentive to understand and predict the flow through the tundish nozzle because its geometry is one of the few variables that is both very influential on the process and relatively inexpensive to change.

Most previous studies have employed water models and plant trials to investigate how nozzle design and operation conditions affect flow in the mold and associated phenomena. Mills and Barnhardt [1] conducted experiments in freezing water models to study the effect of nozzle design on the alumina entrapment mechanism inside the mold cavity. They found an improved flow pattern inside the mold cavity with 4-port nozzles over bifurcated nozzles. Tsai [2] measured pressure below the slide gate in water experiments, and found that proper argon injection might avoid a partial vacuum and hence reduce air aspiration. Dawson [3] investigated inlet curvature and abrupt changes of the nozzle bore using water modeling and steel casting experiments. He found that these geometry changes should be avoided to eliminate flow separation in the nozzle and related problems. Tsukamoto et al. [4] investigated the effects of the inside and bottom shape of the SEN on preventing uneven flow and on decreasing the alumina clogging at the lower part of the SEN by using water model. Gupta and Lahiri [5] performed water modeling experiments for nozzles with different port angles and bore diameters in free-fall and submerged jets. Honeyands et al. [6] performed water modeling experiments for SEN with various bore diameters, port angles and heights and measured the jet angle and the effective port area. Sjöström et al. [7] performed an experimental study of argon injection and the aspiration of air into a stopper rod using liquid steel, and found that air aspiration could be reduced by increasing the argon flow rate or pressurizing the stopper.

Previous mathematical modeling work to investigate how nozzle design and operation conditions affect the nozzle flow pattern and jet properties has been confined mainly to single-phase flow modeling [8-11]. Hershey, Najjar and Thomas performed an extensive parametric study

on single-phase flow in a bifurcated submerged entry nozzle (SEN). They found that the SEN port angle was most influential variable controlling jet angle entering the mold, and the jet always left at a steeper downward than the SEN port angle. Shorter, thicker, and narrower ports forced the flow to conform more closely to the shape of the port walls. They also found that casting speed increased only the jet speed and turbulence levels but did not affect the jet angle or other jet characteristics. Wang [10] formulated a 3-D finite-element model for single-phase flow in a complete nozzle, including the upper tundish well, slide gate and SEN, to study the asymmetrical flow as a result of the slide gate orientation and opening. He found that the 0° slide-gate orientation produced the most uneven flow in the mold, and suggested that the 45° slide-gate orientation improve the symmetry.

The 3-D finite difference model, developed and validated in Part I of this paper, is employed to perform extensive parametric studies to investigate the effects of casting operation conditions (gas injection, slide-gate orientation, casting speed, gate opening and bubble size) and nozzle port geometry (port angle and port shape) on the nozzle flow pattern and jet characteristics. All simulations focus on a typical new bifurcated nozzle with square ports and a condition of no clogging or erosion. The effect of clogging, including both initial clogging and severe clogging is investigated elsewhere[12].

II. COMPUTATIONAL MODEL

A three-dimensional finite difference model was used in this study of time-averaged turbulent flow of molten steel and argon bubbles in slide-gate tundish nozzles. This model is described in detail in Part I of this two-part paper, in which multiphase flow is modeled using the Eulerian multi-fluid model. A separate set of continuity and momentum equations is solved for each of the liquid and gas phases. Coupling is achieved through empirical inter-phase drag forces between the liquid steel and argon bubbles. The standard, two-equation K-ε model is used to account for turbulence in the liquid phase. Based on a grid resolution study, a standard grid was chosen to allow both accurate prediction and economical computing resource. A reliable procedure

to obtain accurate convergence was achieved using proper initial guesses and numerical strategies. The computational model was verified by comparison with measurements using PIV (Particle Image Velocity) technology on a 0.4 scale water model.

Over 150 simulations were performed based on modifications of the standard conditions given in Table I. Only one or two conditions vary during each study in order to isolate the effect of each parameter. The standard nozzle in Table I, has all port edges angled downward uniformly at 15°. Another design used in this work has port angles, which vary around the SEN. The angle of the port edge is 15° downward at the center plane of the wide face, and decreases to 7° downward at the center plane of the narrow face. This port angle is referred to as "non-uniform port angle of 7°-15°". In addition to the nozzle flow pattern, jet characteristics at the port outlets are quantified with weighted-average properties such as jet angle, jet speed, back flow zone and biased mass flow.

III. EFFECT OF ARGON GAS INJECTION

The huge effect of gas injection volume fraction on the flow pattern is illustrated in Figure 1 for a standard nozzle (Table I conditions) but with a 45° gate orientation and non-uniform port angle of 7°-15. Without gas, some low-velocity flow reenters the upper portion of the nozzle ports. This region is thus termed a "back flow" zone. Gas collects at the upper portion of the nozzle ports whenever a back flow zone exists, as shown by the high gas concentration there in Figure 6 of Part I of this paper. For ports with no back flow, such as the nozzle in the validation experiments of Part I, gas collects instead in the central region of the jet swirl. In either case, the gas affects the characteristics of the jet exiting the nozzle.

When gas is injected and the casting speed is kept constant, the flow must accelerate to accommodate the space taken by the gas. This greatly increases the turbulence and changes the vortexing flow or "swirl" pattern exiting the ports. Some of the gas bubbles are carried by the downward jet but most of the bubbles exit from the upper portion of the ports. This second jet is directed upward due to the buoyancy.

The effects of gas injection naturally change with the argon injection flow rate. In general, increasing argon flow rate decreases the vertical jet angle (bends the jet upward), enhances the turbulence level, and reduces the size of the back flow zone. However its effect is greatly altered by other variables such as slide-gate orientation and casting speed. Thus, further quantitative analyses of the effect of argon on jet characteristics are discussed together with these other variables in the next sections.

IV. EFFECT OF SLIDE-GATE ORIENTATION

The slide-gate is used to regulate the steel flow rate by moving horizontally to adjust the opening size. However, the off-center blocking effect generates asymmetric flow that directly affects the flow pattern in the mold. Three typical slide-gate orientations, illustrated in Figure 2, are investigated here. For the 0° gate orientation, the slide-gate moves parallel to the wide face of the mold, so asymmetric jets flow from the left and right outlet ports. For the 90° orientation, the slide-gate moves perpendicular to the wide face of the mold. This avoids obvious asymmetry but generates a strong rotational swirl accompanied by asymmetry in the horizontal plane. This effect was not seen by Wang [10], but is confirmed in water model observations. The 45° orientation is a compromise design between these two extremes.

The simulated flow patterns for the three slide-gate orientations are shown in Figures 3 and 4 for both front and side views, based on the conditions shown in Table I but with a 45° gate orientation and non-uniform port angle of 7°-15. Jet properties at the port outlet are compared in Figures 5-10.

The 0° gate orientation exhibits significant asymmetry between the left and right ports. Specifically, more steel (over 60%) flows from the left port, which is the side opposite to the gate opening. This uneven flow distribution causes biased flow in the mold, with associated quality problems. A much larger back flow zone is found at the right port (32%) than at the left port (11%), and the right port flow is directed slightly steeper downward. Two symmetric small vortices form at the center plane, as shown in Figure 3(b), which diminish by the time the jets exit

the ports. As seen in Figure 4, the time-average jets for the 0° orientation have very little swirl. A high gas concentration collects at the upper portion of the ports. This gas exits the nozzle from the very top of the port, forming a separate upward jet in addition to the main downward jet, which contains very little gas.

The 90° gate orientation generates symmetric flow from the two ports on average, so avoids left-right flow asymmetry in the mold. However, the consistent flow toward the back of the SEN generates a single strong vortex through the entire nozzle. This extends a strong swirl component to the jet leaving both ports. The swirling jets move toward the wide face opposite to the gate opening, as indicated by the positive horizontal jet angle of 3°-4° in Figure 6. Most of the gas exits the nozzle from the very top of the port at the gate opening side, forming a separate upward jet.

The 45° gate orientation creates only a slight improvement to the left-right biased flow through the two ports, relative to the 0° orientation. About 58% liquid flows from the left port. The back flow zone at the right port drops to 24%, but that at the left port stays the same as the 0° orientation (11%). Furthermore, the jet vortex pattern creates jet swirl and flow asymmetries in the horizontal plane that are very close to those found for the 90° orientation configuration. Thus, the 45° orientation appears to have the worst asymmetries of both the 0° and 90° nozzles, with no offsetting improvements. This finding appears to disagree with the conclusion of Wang [10].

The combined effects of slide-gate orientation and gas injection, on the jet are quantified by the weighted-average characteristics at the port, defined in Equations 23-28 in Part I of this paper. The trends are plotted in Figures 5-10. Each point on those plots represents one simulation performed on the standard nozzle for operation conditions in Table I, except for the gas flow rate and the slide-gate orientation.

A. Vertical jet angle

The vertical jet angle measures the direction of the overall average jet flow. A positive vertical jet angle corresponds to a downward jet. It is noticed in Figure 5 that the vertical jet angle is very close to the port angle when there is no gas injected. With increasing gas injection, the gas buoyancy bends the average jet upward. This observation is almost independent of gate orientation and differs from the findings of previous single–phase flow modeling [8] that the jet angle is always much steeper downward than the port angle. In addition to the presence of gas, the present findings are likely due to the shallower port height and the increased port thickness of the standard nozzle geometry.

Increasing the gas flow rate gives buoyancy to the jet, so it is directed less downward when it leaves the nozzle. This is quantified by the decrease in vertical jet angle from 15° to 5°, seen in Figure 5. The left and right ports are about the same for the 90° orientation nozzle. For the 0° and 45° orientations without gas, however, the vertical jet angles at the left port are slightly shallower than at the right port (on the gate opening side). Increasing gas injection tends to reduce this asymmetry.

B. Horizontal jet angle

The horizontal jet angle indicates how far the average jet flow deviates from the center plane. A positive horizontal jet angle corresponds to a deviation toward the wide face opposite from the gate opening, as shown in Figure 2. The largest horizontal jet angle occurs at the left port of the 45° orientation without gas. This asymmetry decreases slightly with increasing gas flow rate.

For the 0° orientation, the average horizontal jet angle is always zero due to symmetry, although the jet spreads slightly as it leaves the port. The 90° and 45° orientation configurations have significant horizontal jet angles due to the strong swirling vortex. On average, the flow is directed toward the wide face opposite to the gate opening. For a typical slab of 0.203m x 1.321m,

the jet centerline will still impinge on the narrow face even for the worst asymmetry (5.3°), unless the swirl causes additional asymmetry in the mold cavity.

C. Jet speed

The jet speed is the weighted average of the liquid velocities flowing out of the port, as defined in Equation 27 of Part I of the paper and plotted in Figure 7. For a given liquid flow rate, the jet speed increases with increasing size of back flow zone. Thus, for the 0° and 45° orientations, the jet speed at the right port is larger than at the left port. The jet speed is the smallest for the 90° orientation and largest for the 0° orientation. Figure 7 also shows that jet speed increases slightly with increasing gas flow rate. This is because the gas volume leaves less space available for the liquid, for a given liquid flow rate.

D. Back-flow zone fraction

The back-flow zone fraction is the area of the nozzle port where flow reenters the nozzle relative to the total port area. This region is found at the upper portion of most nozzle ports. Figure 8 shows that the back-flow fractions at the left port are much smaller than at the right port for 0° and 45° orientations. The larger back-flow zone develops at the gate opening side. The back-flow fraction decreases slightly with increasing gas flow rate.

It was observed in water modeling [10] that unsteady periodic pulsing of the jets at the ports increases with larger back flow zones. This may increase surface level fluctuations and other problems in the mold.

E. Biased mass flow

Biased or asymmetric flow refers to the difference in mass flow rate from the two ports. Figure 9 shows the liquid and gas mass flow percentages out of the left port, which is due to the off-center throttling effect of the slide-gate.

The 0° gate orientation naturally generates the most biased mass flow with over 60% of the liquid leaving the left port. The 90° orientation naturally has an unbiased 50% from each port. This

agrees with Wang's observation for single-phase flow [10]. About 58% of the liquid exits the left port for all 45° orientation cases modeled. This negligible improvement contrasts with the improvement reported by Wang for the 45° gate [10] and suggests that the effect of orientation on the biased mass flow might vary with nozzle design. Gas injection has very little influence on the biased liquid flow, although the gas flow becomes more symmetrical.

F. Turbulence kinetic energy

The turbulence of the jets increases with gas injection, as shown by the average turbulent kinetic energy K results in Figure 10. The highly swirling jets of the 90° orientation generate the largest K of the three orientations. The average turbulence dissipation rates ε (not shown) have the same trends as K.

V. EFFECT OF CASTING SPEED

Increasing casting speed was investigated by performing simulations at 1.5m/min and 2.3m/min, in addition to the standard casting speed (1m/min) in Table I. All casting speeds refer to a 0.203m x 1.321m slab. All simulated cases here have the 45° gate orientation (45°), fixed gate opening (F_L=50%) and same non-uniform port angle of 7°-15°. Casting speed can be adjusted by changing either slide-gate opening or tundish bath depth. Therefore, the casting speed changes discussed here are achieved by adjusting the liquid head in the tundish. Slide-gate opening effects are address independently in the next section. Increasing casting speed also requires the gas flow rate to increase in order to maintain a given gas fraction. The combined effects of casting speed and gas injection on the jet are quantified in Figures 11-16, which plot the weighted-average jet characteristics.

For single-phase flow, the casting speed has little influence on the flow pattern and its associated jet characteristics such as vertical jet angle, horizontal jet angle, back flow zone and biased mass flow. This is shown by the common intercepts at zero gas volume fraction in Figures 11, 12, 14, and 15. Jet speed and turbulence energy naturally increase with casting speed, as

shown in Figures 13 and 16. These findings agree with previous single-phase flow studies [8, 9] and tend to justify the common practice of scale water models.

With increasing gas injection, the vertical jet angle becomes shallower due to the gas buoyancy. The horizontal jet angle and back flow zone also decrease. These effects of the gas become less influential with increasing casting speed, as shown in Figures 11, 12 and 14. This is likely because the liquid momentum tends to dominate more over buoyancy as the liquid flow rate increases. Neither casting speed nor gas injection have much influence on biased liquid mass flow, as seen in Figure 15. Increasing casting speed produces a steeper downward jet angle, larger horizontal jet angle, larger back flow zone, higher casting speed and stronger turbulence, even for a constant gas fraction, where gas flow rate increases in proportion with the casting speed.

VI. EFFECT OF SLIDE-GATE OPENING

Five different gate opening fractions are simulated in this parametric study, ranging from 40% linear opening (F_L=40%) to full opening (F_L=100%). The slide gate opening fraction F_L is a linear fraction of the opening distance, and is defined as the ratio of the displacement of the throttling plate (relative to the just-fully closed position) to the bore diameter of the SEN. This popular measure can be converted to the more fundamental gate opening definition of area fraction, F_A, via

$$F_A = \frac{2}{\pi}\cos^{-1}\left(1-F_L\right) - \frac{2}{\pi}\left(1-F_L\right)\sqrt{1-\left(1-F_L\right)^2} \qquad (1)$$

The five simulations used to plot jet characteristics in Figure 17 all have the geometry and conditions of the standard nozzle in Table I except for the gate opening. It should be noted that all cases are run with the same casting speed in the absence of clogging or erosion. In practice, the gate opening is adjusted to compensate for these and other variations in order to maintain a constant liquid level in the mold. The effect of clogging is investigated elsewhere [12].

The horizontal jet angle decreases with increasing gate opening, and approaches zero as the opening approaches 100%, as shown in Figure 17(a). This is natural because the off-center blocking effect decreases as the gate opening approaches the symmetrical full open condition. All

other jet characteristics are found to have maximum or minimum values near the gate opening of F_L=60% (50% area fraction). At this critical opening fraction, the vertical jet angle is steepest downward, the back flow zone is largest and turbulence at the port is lowest. In addition, the pressure drop below the slide gate that leads to detrimental vacuum conditions is most severe [12].

VII. EFFECT OF BUBBLE SIZE

The effect of bubble size was investigated by increasing bubble diameter from 1mm to 3mm and 5 mm for the standard nozzle and conditions in Table I. Important jet characteristics are compared in Figure 18.

Larger bubbles cause a shallower vertical jet angle. This is due to their greater buoyancy despite their smaller numbers for a given gas fraction. This effect becomes more significant at higher argon flow rate. Through this effect, bubble size variations could readily cause flow fluctuations in the mold. The horizontal jet angle increases only slightly with increasing bubble size. Bigger bubbles tend to reduce the size of the back flow zone but enhance turbulence, especially at high gas flow rate.

A study of bubble formation [13] shows that the average bubble size depends mainly on the gas injection flow rate at the local pore on the inner wall of the nozzle and the downward liquid velocity. The bubble size increases and the size distribution becomes less uniform as the liquid velocity and gas flow rate increase. Modeling of two-phase flow shows that the bubble size also affects the flow pattern in the mold [14-16]. Large bubbles tend to rise immediately to the free surface but small bubbles tend to follow the liquid flow and penetrate deeper into the caster, where they may be entrapped by the solidified shell, leading to blisters and other defects [13].

VIII. EFFECT OF NOZZLE PORT DESIGN

The effects of nozzle design parameters, including the angle, shape, height, width and thickness of the ports on the nozzle flow pattern and jet characteristics have been reported

previously for single-phase flow with finite element models [9]. A parametric study here investigates the effect of port angle and rectangular port shape with argon gas injection.

A. Nozzle port angle

Three different vertical angles of the upper and lower port edges (15° up, 15° down and 25° down) are simulated for the standard nozzle and conditions in Table I. Figure 19 compares the predicted flow patterns viewing into the wide face and into the left outlet port, and the jet characteristics are plotted in Figure 20. It can been seen that a steeper downward port angle generates a steeper downward jet angle. This is consistent with previous finding without gas [8, 9]. The vertical jet angle is consistently a few degrees more upward than the port angle, owing to the gas buoyancy. Without gas, the jet angle is more downward than the port angle, although for this nozzle geometry, the difference was very slight.

Gas is seen to collect in the upper right portion of the port outlet in and near the back flow region. The back flow zone is larger with shallower port angles. With 25° down ports, the back flow zone disappears and the average horizontal jet angle is almost zero. Turbulence energy is unaffected by port angle.

B. Nozzle port shape

Three different port shape designs (78mmx78mm square, 64mmx95mm rectangle, and 55mmx122mm slender rectangle) are simulated for the standard nozzle and conditions in Table I. All three designs have the same port area and same port angle (15° downward). The flow patterns are compared in Figure 21 and the jet characteristics in Figure 22.

Port shape greatly changes the vertical jet angle. The square port generates the shallowest jet. The jet from the rectangular (64x95) port is angled about the same as the port angle. The slender rectangle (50x122) port produces a very steep downward jet (27.8°down) despite the high gas injection rate (16%). All three designs have small horizontal jet angles (< 3°) which decrease slightly as the port shape becomes more slender. The square port allows the strongest swirl to exit the port, leading to the most asymmetry in the mold, as shown by the larger horizontal jet angle. The square port also splits off the largest upward gas-rich jet, and has the largest back flow zone

and jet speed. Both rectangle port designs have much smaller back flow zones, and single swirls covering over 90% of the port area. The slender rectangle port has a slightly larger back flow zone than the rectangular port.

IX. PRESSURE DROP APPLICATION

The pressure drop along the nozzle is greatest at the slide gate and can be output from the model results. Figure 23(a) shows the effect of gas flow and gate orientation on pressure drop across the entire nozzle from the tundish bottom to the submerged ports. It can be seen that the gate orientation has very little influence on the pressure drop. The pressure drop increases linearly with increasing gas fraction. This is due to the resistance to the downward flow caused by the gas buoyancy. The flow resistance naturally also increases with increasing liquid flow rate and decreasing gate opening. Thus, the pressure drop increases with higher casting speed for a fixed gate opening, as shown in Figure 23(b), and decreases with increasing gate opening for a fixed casting speed, as shown in Figure 23(c). The pressure solutions from other simulations reveal that the pressure drop over the nozzle is generally independent of bubble size, port angle and port shape, even though these parameters can greatly change the flow pattern and jet characteristics.

The pressure drop across the nozzle can be related to the tundish bath depth [12, 17]. The relationship is complicated, however, because casting speed, gate opening, gas injection and tundish bath depth are all inter-related. The present parametric studies vary only one of the three variables: casting speed, gate opening, and gas injection at a time, keeping the other two constant. This corresponds to simultaneous variation of tundish bath depth, which is unknown in practice. In work reported elsewhere [12, 17], tundish bath depth and argon injection are kept constant, and gate opening is regulated according to casting speed.

In addition to affecting the relationship between casting speed, gate opening, gas injection and tundish depth, the pressure drop across the nozzle is important to air aspiration, which leads to reoxidation, nozzle clogging and defect formation. If the ceramic walls are porous, or leaks develop between the sliding gates, then air can be aspirated into the nozzle if the gage pressure

becomes negative. These simulations predict that the pressure does indeed drop below 1 atmosphere for many simulations and the minimum pressure is found just below the slide gate. This is affected by gas injection. The results presented here are applied in related work to predict this condition [12, 17].

X. MOLD FLOW APPLICATION

Flow in the liquid pool in the mold can be modeled separately from the nozzle to simplify the calculation [14, 15, 18-20]. The nozzle port is then the inlet boundary of the mold domain. The inlet boundary condition for these mold simulations can be obtained from the corresponding nozzle simulation results presented here.

There are three ways to implement this boundary condition and achieve the desired one-way coupling of the nozzle model to a mold simulation. First, the overall average jet characteristics, defined in Equations 23-28 in Part I of this paper, can be directly imposed as uniform conditions over the inlet boundary. Specifically, a uniform velocity fixed at the average jet speed can be specified on an inlet region fixed to the out flow portion of the lower part of the nozzle outlet port and directed according to the average vertical and horizontal jet angles. In addition, the turbulence energy K, dissipation ε, over the inlet can be fixed according to the weighted average values for the jet specified in this work. A uniform gas volume fraction can be imposed over the inlet boundary. This simple method is a reasonable approximation, especially for flows with low gas fractions and little swirl component, such as found in the 0° gate orientation or stopper-rod nozzles. For these cases, the upper portion of the port is usually pure back flow.

For those cases with two separate jets on the same port, which are often found for the 45° or 90° gate orientation with high gas flow rate, values calculated for a split-jet can be used for the mold flow simulation, as described in Part I of this paper. The nozzle port area is divided into 3 separate inlet areas for the gas-rich upward jet, the liquid-rich downward jet, and a middle section for the back flow zone. The size of each region depends on the area occupied by the corresponding jet. Uniform average jet properties for the upward jet are specified on the upper jet inlet section,

and those for the downward jet are specified on the lower section. The slow moving back flow zone can be ignored.

For complex nozzle exit flows where additional accuracy is desired, another method is to impose the nozzle simulation results directly onto the inlet domain for the mold calculation. Individual velocity components for liquid and gas, volume fraction, and turbulence properties can be defined for each cell on the port using a user subroutine and swirl can be incorporated. Each of these three methods avoids the significant extra complexity and expense of combining the nozzle and mold geometry together as a single computation.

XI. CONCLUSIONS

A three-dimensional finite difference model, developed and verified in Part I of this paper, is employed to study steady turbulent flow of liquid steel and argon bubbles in slide-gate tundish nozzles. Parametric studies are performed to investigate the effects of casting operation conditions (gas injection, slide-gate orientation, casting speed, gate opening and bubble size) and nozzle port design (port angle and port shape). The effects on the flow pattern and gas distribution in the nozzle are examined. The effects on the jet characteristics at port outlet are quantified using weighted average jet angle, jet speed, back flow zone fraction, turbulence and biased mass flow. The main observations are summarized below.

- Gas injection greatly affects the flow pattern and jet characteristics. Increasing gas injection bends the jet upward, enhances turbulence, and reduces the back flow zone size. A few gas bubbles are carried by the downward liquid jet while most gas exits the nozzle from the upper portion of the ports, forming a separate upward jet due to the gas buoyancy.
- Gas injection becomes less influential with increasing casting speed.
- For single-phase flow, casting speed has little influence on flow pattern characteristics such as vertical jet angle, horizontal jet angle, back flow zone and biased mass flow.
- The off-center blocking effect of the slide-gate generates asymmetric flow.

- The 0° gate orientation generates the worst biased flow between the left and right ports. Specifically, the port on the gate opening side has a steeper jet angle, much larger back flow zone and less than 40% of the liquid mass flow.
- The 90° gate orientation generates strong swirl and asymmetry in the horizontal plane, with a horizontal jet angle that directs the average jet toward the wide face opposite the gate opening side.
- The 45° gate orientation has all the asymmetries of both the 0° and 90° design, so appears to be a poor compromise.
- The horizontal jet angle decreases with increasing gate opening, and becomes zero when fully open.
- The vertical jet angle, jet speed and back flow zone size reach their maximum values near gate opening F_L=60% (50% area fraction), and decrease as the gate opening moves away from this critical value.
- Increasing gas injection seems to reduce the asymmetry slightly, so long as the bubble size stays constant. Larger bubbles have more influence on the flow pattern for a given gas fraction due to their greater buoyancy.
- Higher gas injection could influence flow in ways not easy to predict from this work.
- The vertical jet angle becomes steeper with steeper port angle or more slender port shape.
- Pressure drop across the nozzle increases with increasing gas injection, increasing casting speed, and decreasing gate opening. However, pressure drop is insensitive to slide-gate orientation, bubble size and port design.

ACKNOWLEDGMENTS

The authors wish to thank the National Science Foundation (Grant #DMI-98-00274) and the Continuous Casting Consortium at UIUC, including Allegheny Ludlum, (Brackenridge, PA), Armco Inc. (Middletown, OH), Columbus Stainless (South Africa), Inland Steel Corp. (East Chicago, IN), LTV Steel (Cleveland, OH), and Stollberg, Inc., (Niagara Falls, NY) for their continued support of our research, AEA technology for use of the CFX4.2 package and the National Center for Supercomputing Applications (NCSA) at the UIUC for computing time.

NOMENCLATURE

F_A	slide-gate opening (area fraction, Equation 1)
F_L	slide-gate opening, linear fraction
f_g	average gas volume fraction (“hot” argon in steel)
Q_G	“cold” argon gas flow rate, measured at 25˚C and 1 atmosphere (SLPM)
V_C	casting speed, based on 0.203m x 1.321m slab (m/min)

REFERENCES

1. Mills, N.T. and Barnhardt, L.F., "The development of submerged entry tundish nozzles," Journal of Metals, vol. 23 (11) (1971), pp. 37-43.
2. Tsai, H.T., "Water Modeling on Pressure Profile in the Tundish Shroud at Flo-Con", private communication, Inland Steel, 1986.
3. Dawson, S.M., "Tundish Nozzle Blockage During the Continuous Casting of Aluminum-killed Steel" (Paper presented at 73rd Steelmaking Conference, Detroit, MI, 1990, Iron and Steel Society, Inc.), vol. 73, pp. 15-31.
4. Tsukamoto, N., Ichikawa, K., Iida, E., Morita, A., Inoue, J., "Improvement of submerged nozzle design based on water model examination of tundish slide gate" (Paper presented at 74th Steelmaking Conference, 1991, Iron and Steel Society), vol. 74, pp. 803-808.

5. Gupta, D. and Lahiri, A.K., "Water modelling study of the jet characteristics in a continuous casting mould," vol. 63 (5) (1992), pp. 201-204.

6. Honeyands, T., Lucas, J., Chambers, J., Herberston, J., "Preliminary modelling of steel delivery to thin slab caster moulds" (Paper presented at 75th Steelmaking Conference, Toronto, Canada, 1992, Iron and Steel Society-AIME), vol. 75, pp. 451-459.

7. Sjöström, U., Burty, M., Gaggioli, A., Radot, J., "An Experimental Study of Argon Injection and Aspiration of Air into Stopper Rod in Continuous Casters" (Paper presented at 81st SteelMaking Conference, Toronto, Canada, 1998, Iron and Steel Society, Inc.), vol. 81, pp. 63-71.

8. Hershey, D., Thomas, B.G. and Najjar, F.M., "Turbulent Flow through Bifurcated Nozzles," International Journal for Numerical Methods in Fluids, vol. 17 (1) (1993), pp. 23-47.

9. Najjar, F.M., Thomas, B.G. and Hershey, D., "Numerical Study of Steady Turbulent Flow through Bifurcated Nozzles in Continuous Casting," Metallurgical Transactions B, vol. 26B (4) (1995), pp. 749-765.

10. Wang, Y.H., "3-D Mathematical Model Simulation on the Tundish Gate and Its Effect in the Continuous Casting Mold" (Paper presented at 10th Process Technology Conference, Toronto, Ontario, Canada, 1992, Iron and Steel Society, Inc.), vol. 75, pp. 271-278.

11. Yao, M., "Flow Simulation of Molten Steel for Immersion Nozzle Design in Continuous Casting Process" (Paper presented at Modeling and Control of Casting and Welding Processes IV, 1988, TMS), pp. 893-898.

12. Bai, H. and Thomas, B.G., "Effects of Clogging, Argon Injection and Tundish Depth on Flow Rate and Air Aspiration in Submerged Entry Nozzles" (Paper presented at 83rd Steelmaking Conference, Pittsburgh, PA, 2000, Iron and Steel Society, Warrendale, PA), vol. 83, pp. 183-197.

13. Thomas, B.G., Dennisov, A. and Bai, H., "Behavior of Argon Bubbles during Continuous Casting of Steel" (Paper presented at 80th ISS Steelmaking Conference, Chicago, 1997), pp. 375-384.

14. Thomas, B.G. and Huang, X., "Effect of Argon Gas on Fluid Flow in a Continuous Slab Casting Mold" (Paper presented at 76th Steelmaking Conference, Dallas, TX, 1993, Iron and Steel Society), vol. 76, pp. 273-289.

15. Thomas, B.G., Huang, X. and Sussman, R.C., "Simulation of Argon Gas Flow Effects in a Continuous Slab Caster," Metallurgical Transactions B, vol. 25B (4) (1994), pp. 527-547.

16. Creech, D., "Computational Modeling of Multiphase Turbulent Fluid Flow and Heat Transfer in the Continuous Slab Casting Mold" (MS Thesis, University of Illinois at Urbana-Champaign, 1999).

17. Bai, H. and Thomas, B.G., "Two Phase Flow in Tundish Nozzles during Continuous Casting of Steel" (Paper presented at Materials Processing in the Computer Age III, TMS Annual Meeting, Nashville, TN, 2000), pp. 85-99.

18. Sivaramakrishnan, S., Bai, H., Thomas, B., Vanka, P., Dauby, P., Assar, M., "Transient Flow Structures in Continuous Casting of Steels" (Paper presented at 59th Ironmaking Conference, Pittsburgh, PA, 2000, Iron and Steel Society, Warrendale, PA), vol. 59, pp. 541-557.

19. Thomas, B.G., Mika, L.M. and Najjar, F.M., "Simulation of fluid flow inside a continuous slab casting machine," Metallurgical Transactions B, vol. 21B (2) (1990), pp. 387-400.

20. Thomas, B.G. and Najjar, F.M., "Finite-Element Modeling of Turbulent Fluid Flow and Heat Transfer in Continuous Casting,," Applied Mathematical Modeling, vol. 15 (May) (1991), pp. 226-243.

FIGURE AND TABLE CAPTIONS

Table I Standard nozzle dimension and operation conditions

Figure 1 Effect of argon gas injection on flow pattern in the nozzle (a) no gas (b) 16% gas (V_C=1m/min, F_L=50%, 45° orientation)

Figure 2 Slide-gate orientation (top view) showing horizontal jet angle

Figure 3 Flow field at the center planes under different gate orientation (a) center plane parallel to wide face (b) center plane parallel to narrow face (V_C=1m/min, Q_G=10SLPM, f_l=16%, F_L=50%,)

Figure 4 Flow field at the nozzle ports for different slide gate orientations (V_C=1m/min, Q_G=10SLPM, f_l=16%, F_L=50%,)

Figure 5 Effects of slide-gate orientation and gas injection on vertical jet angle

Figure 6 Effects of slide-gate orientation and gas injection on horizontal jet angle

Figure 7 Effects of slide-gate orientation and gas injection on jet speed

Figure 8 Effect of slide-gate orientation and gas injection on back flow zone

Figure 9 Effect of slide-gate orientation and gas injection on biased mass flow

Figure 10 Effect of the slide-gate orientation and gas injection on turbulence energy

Figure 11 Effects of casting speed and gas injection on vertical jet angle

Figure 12 Effects of casting speed and gas injection on horizontal jet angle

Figure 13 Effects of casting speed and gas injection on jet speed

Figure 14 Effects of casting speed and gas injection on back flow zone

Figure 15 Effects of casting speed and gas injection on biased mass flow

Figure 16 Effects of casting speed and gas injection on turbulence energy

Figure 17 Effects of gate opening on (a) jet angles, (b) jet speed and back flow zone, and (c) turbulence energy and dissipation

Figure 18 Effect of argon bubble size and gas injection on (a) vertical and horizontal jet angles, and (b) back flow zone and turbulence energy (V_C=1m/min, F_L=50%, 90° orientation)

Figure 19 Liquid velocity fields superimposed on liquid volume fraction at center plane and port under different nozzle port angles (a)15° up (b) 15° down (c) 25° down (V_C=1m/min, Q_G=10SLPM, f_g=16%, F_L=50%, 90° orientation)

Figure 20 Effect of the port angle on (a) vertical and horizontal jet angles, and (b) back flow zone and turbulence energy (V_C=1m/min, Q_G=10SLPM, f_l=16%, F_L=50%, 90° orientation)

Figure 21 Liquid velocity fields superimposed on liquid volume fraction at center plane and port under different port shape designs (V_C=1m/min, Q_G=10SLPM, f_g=16%, F_L=50%, 90° orientation)

Figure 22 Effect of port shape design on (a) Vertical jet angles (b) Horizontal jet angle (c) Jet speed (d) Back flow zone ratio (V_C=1m/min, F_L=50%, 90° orientation, 15° port angle)

Figure 23 Effects of (a) gas injection and slide-gate orientation, (b) casting speed, and (c) slide-gate opening and on pressure drop across the nozzle

Table I Standard nozzle dimensions and operation conditions

Parameter	Standard Nozzle	
	SI Units	British units
Total nozzle length	1152.5 mm	45.37 in.
UTN top diameter	114 mm	4.49 in.
UTN length	241.5 mm	9.51 in.
Slide gate thickness	63 mm	2.48 in.
Slide gate diameter	78 mm	3.07 in.
Shroud holder thickness	100 mm	3.94 in.
SEN length	748 mm	29.45 in.
SEN bore diameter	78 mm	3.07 in.
SEN submerged depth	200 mm	7.87 in.
Port width x height	78mm x 78mm	3.07″ x 3.07″
Port thickness	29 mm	1.14 in.
Port angle (down)	15°	15°
Recessed bottom well depth	12 mm	0.47 in.
Gate orientation	90°	90°
Gate opening Linear fraction (F_L) Area fraction (F_A)	 50% 39%	 50% 39%
Casting speed (0.203m x 1.321m slab)	1.0 m/min	39.4 in./min (8″x52″slab)
Liquid flow rate	268.4 l/min	9.48 ft^3/min
Argon injection flow rate Q_G (cold)	10 SLPM	0.35 SCFM
Argon injection (hot) volume fraction	16%	16%
Argon bubble diameter	1.0 mm	0.039 in.

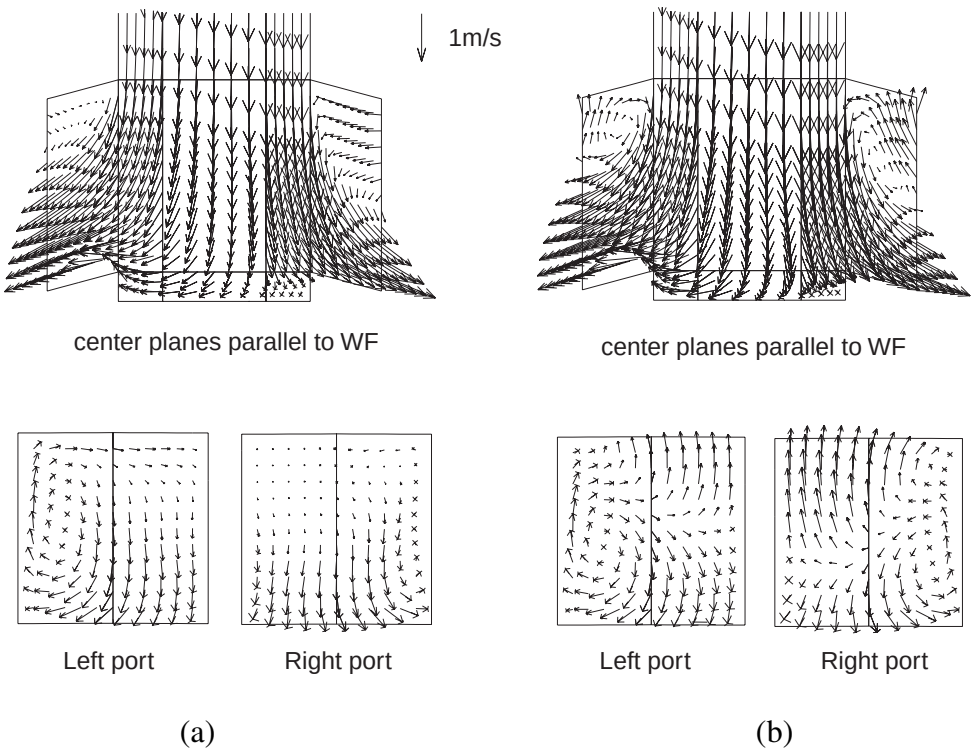

Figure 1 Effect of argon gas injection on flow pattern in the nozzle (a) no gas (b) 16% gas (V_C=1m/min, F_L=50%, 45° orientation)

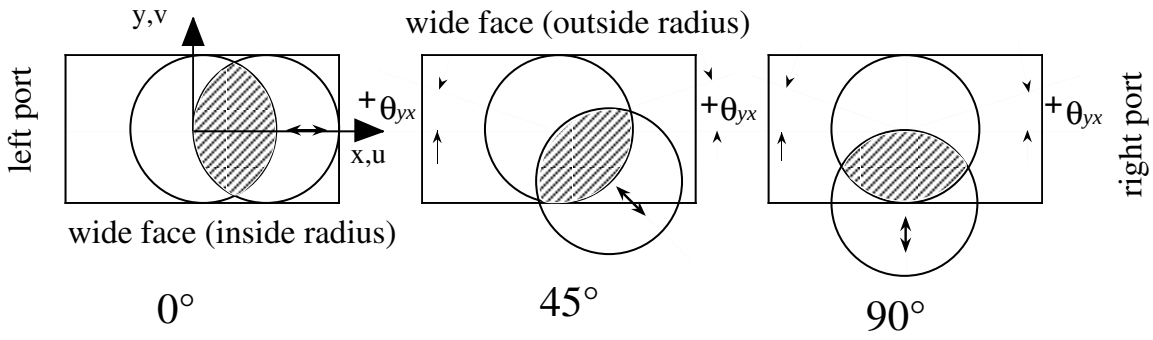

Figure 2 Slide-gate orientation (top view) showing horizontal jet angle

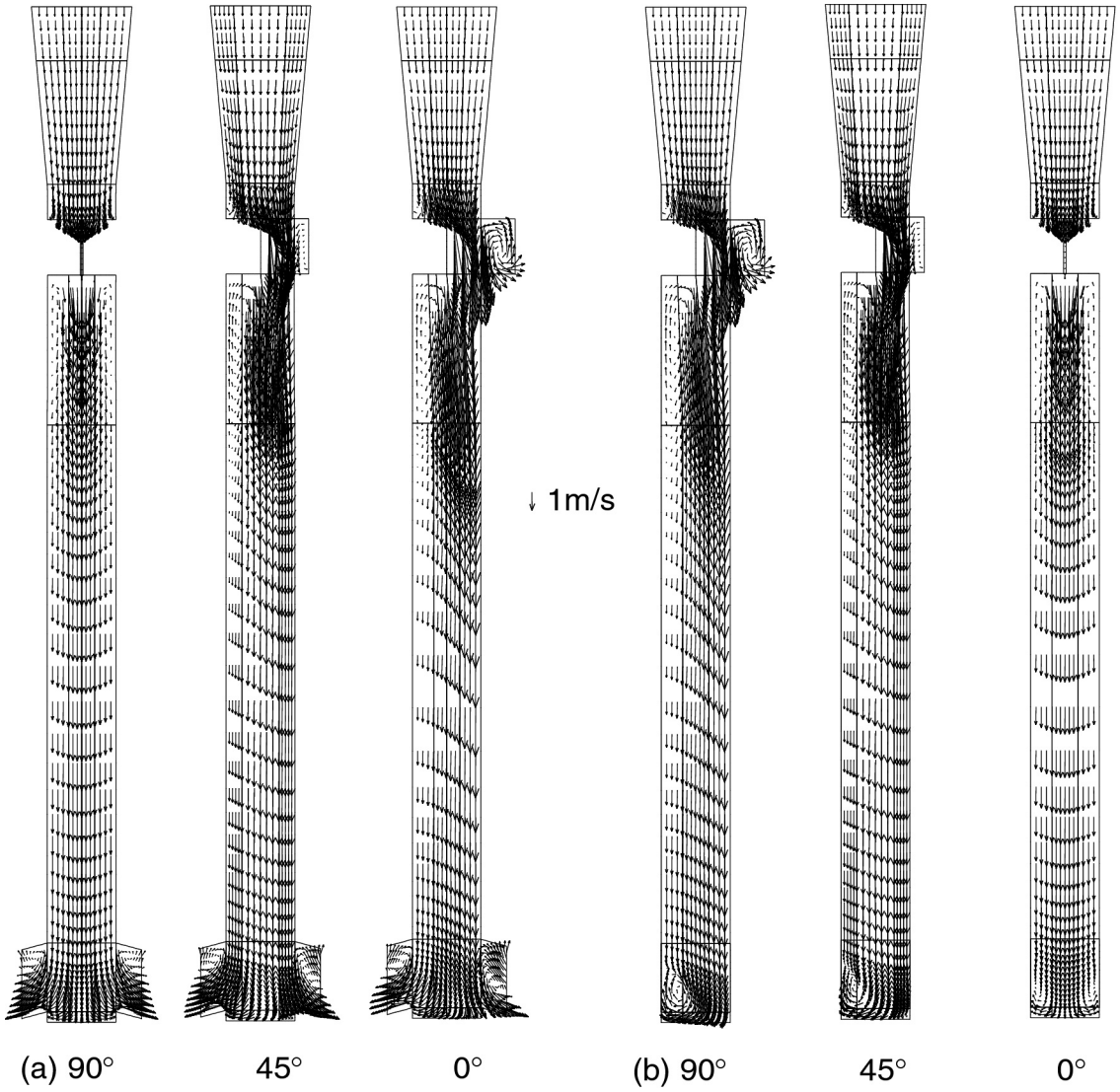

Figure 3 Flow field at the center planes for different gate orientations
(a) center plane parallel to wide face (b) center plane parallel to narrow face
(V_C=1m/min, Q_G=10SLPM, f_l=16%, F_L=50%,)

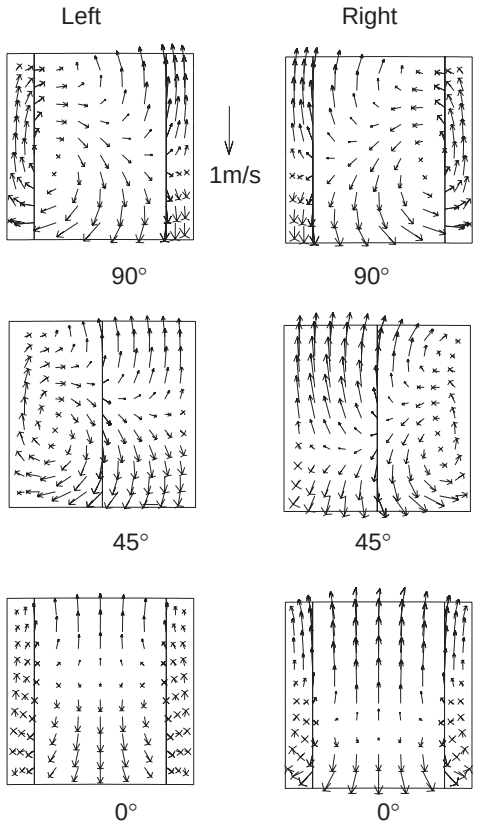

Figure 4 Flow field at the nozzle ports for different slide gate orientations
(V_C=1m/min, Q_G=10SLPM, f_l=16%, F_L=50%,)

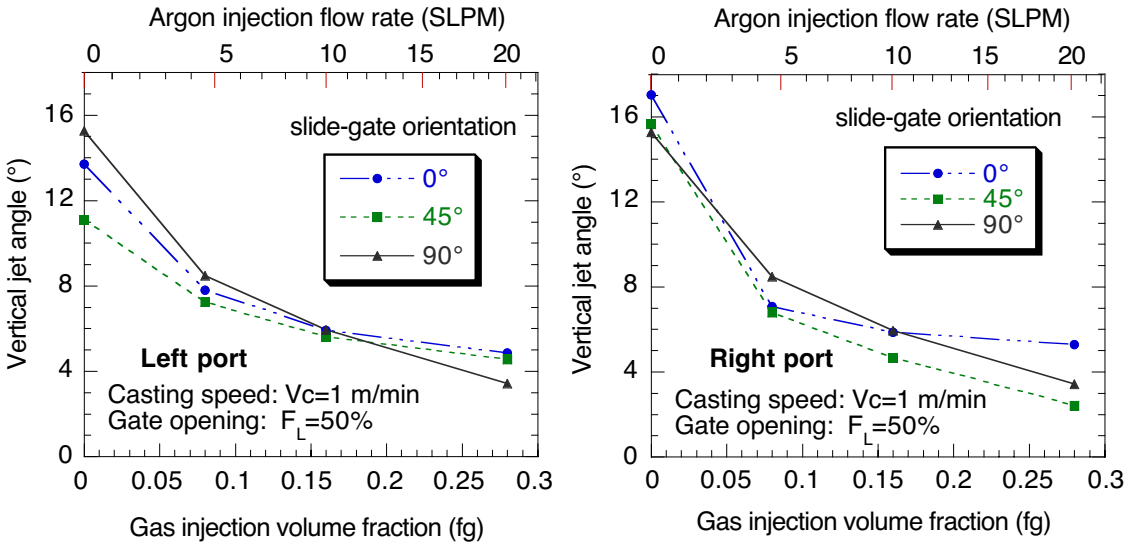

Figure 5 Effects of slide-gate orientation and gas injection on vertical jet angle

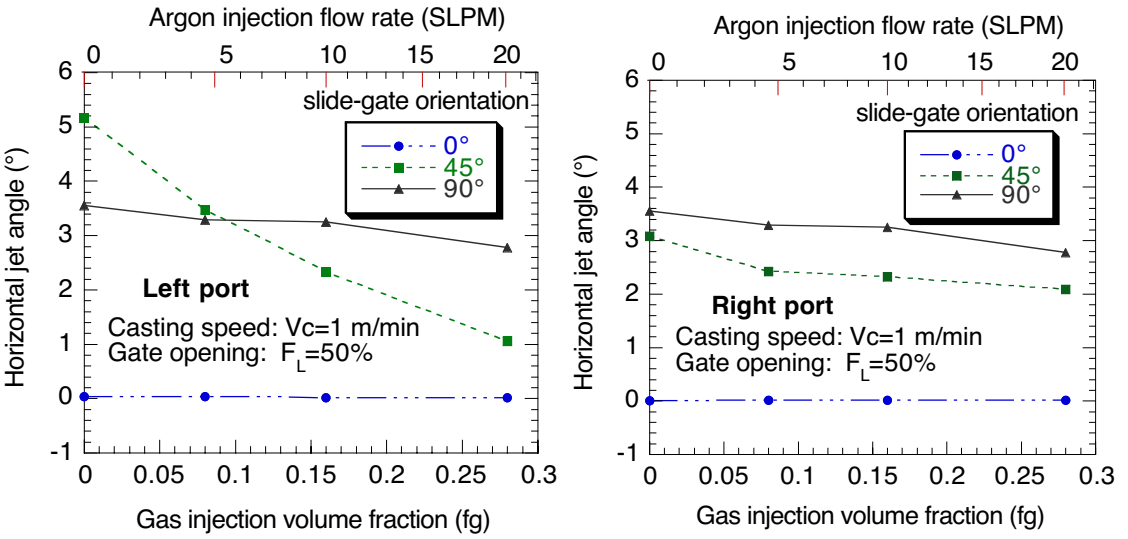

Figure 6 Effects of slide-gate orientation and gas injection on horizontal jet angle

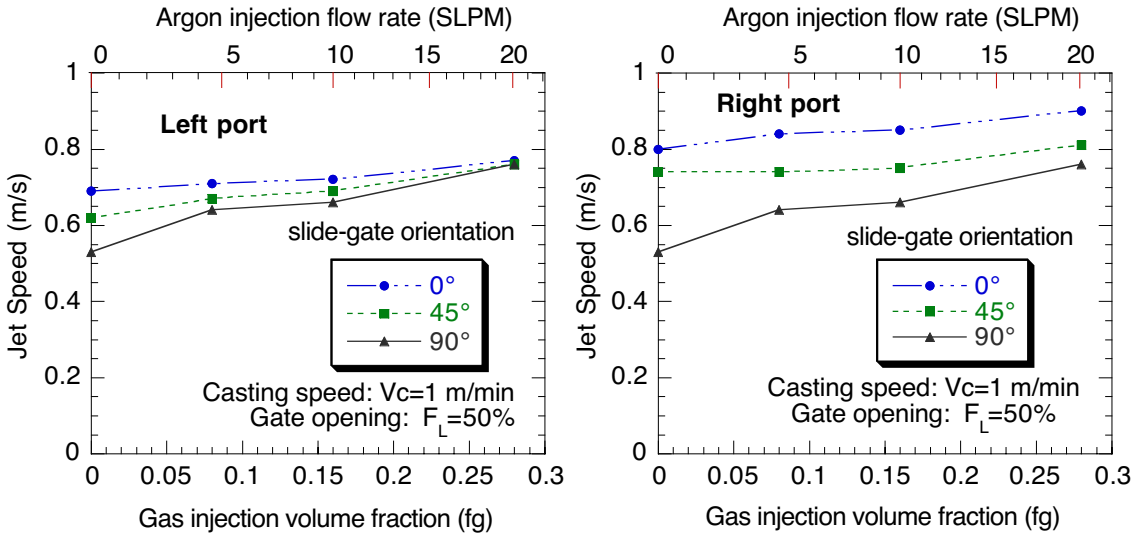

Figure 7 Effects of slide-gate orientation and gas injection on jet speed

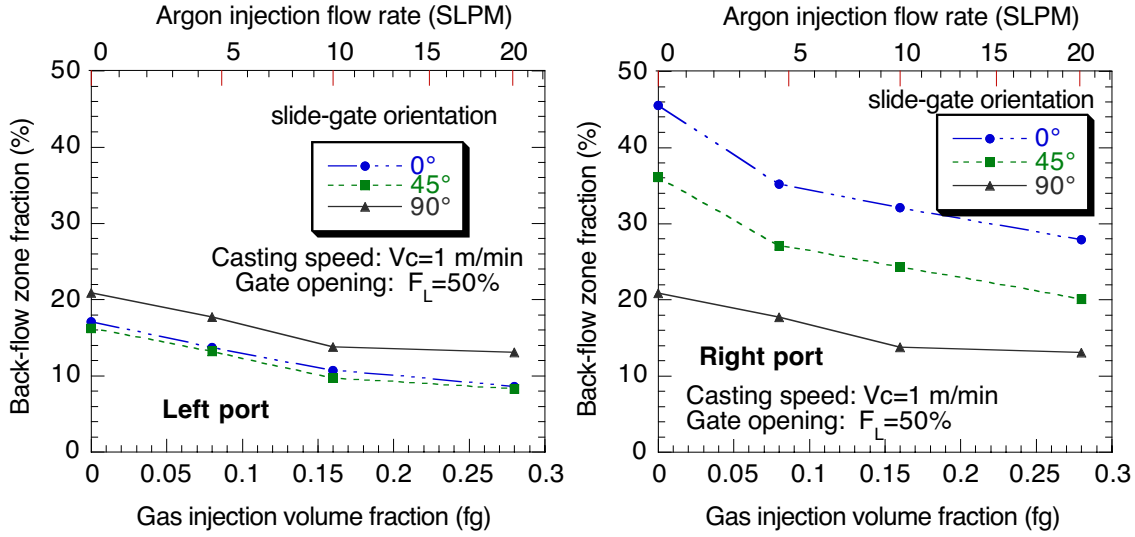

Figure 8 Effect of slide-gate orientation and gas injection on back flow zone

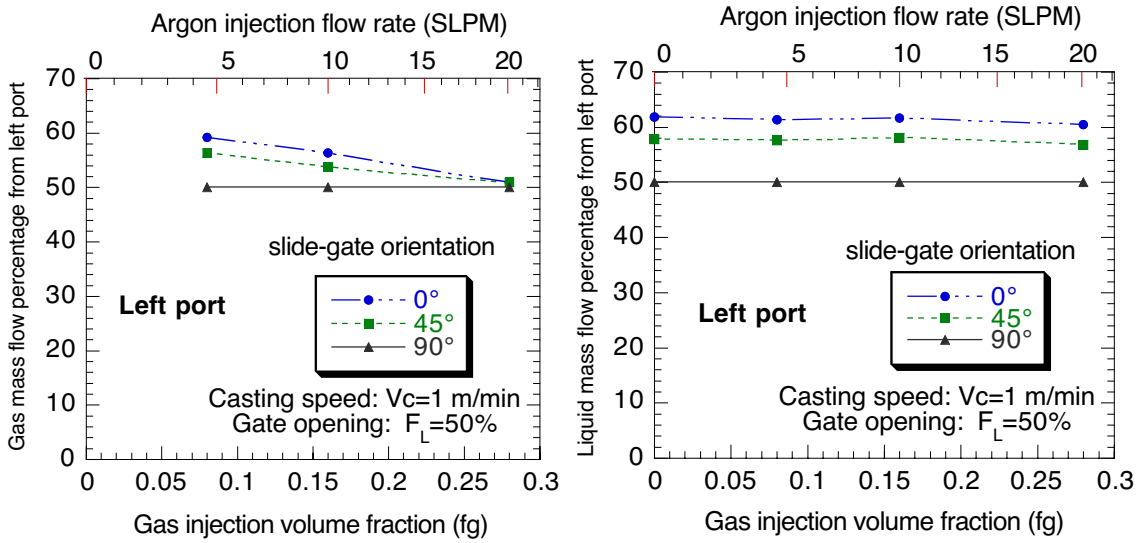

Figure 9 Effect of slide-gate orientation and gas injection on biased mass flow

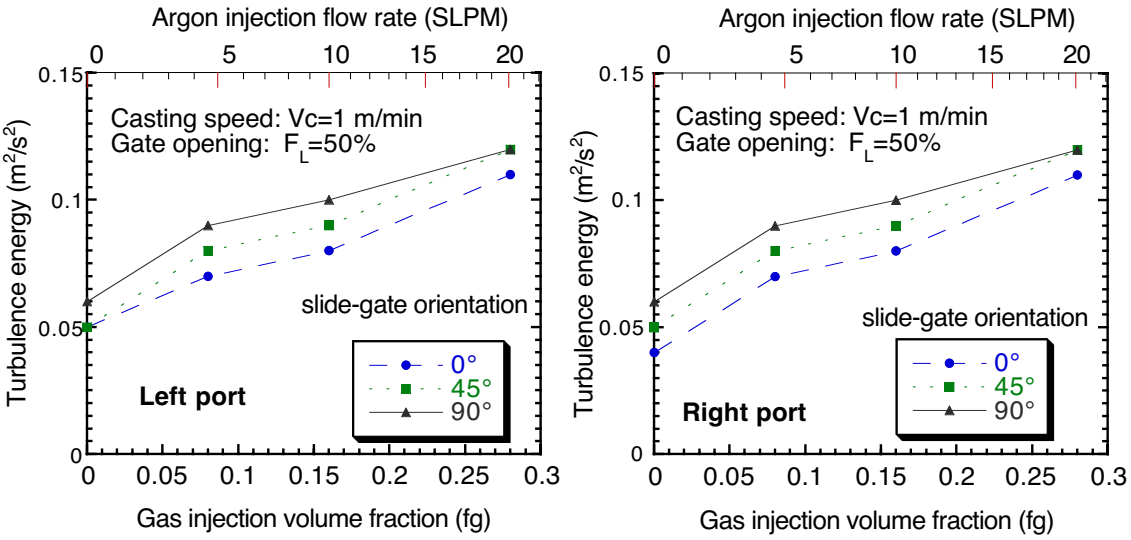

Figure 10 Effect of slide-gate orientation and gas injection on turbulence energy

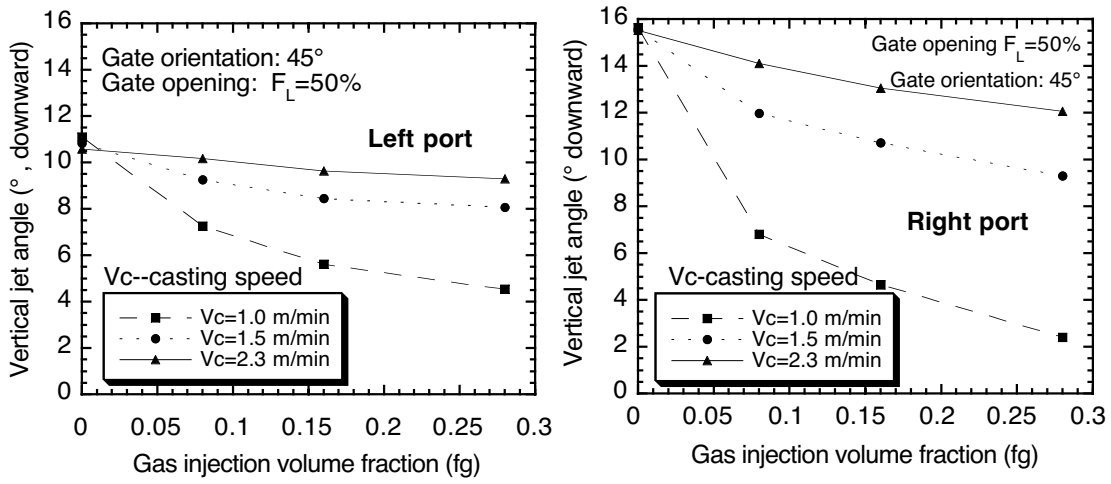

Figure 11 Effects of casting speed and gas injection on vertical jet angle

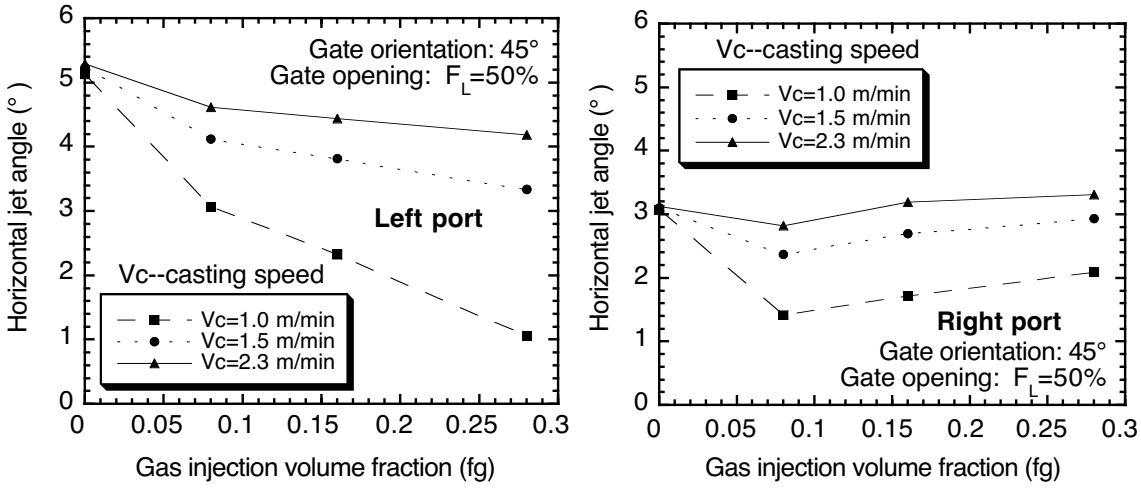

Figure 12 Effects of casting speed and gas injection on horizontal jet angle

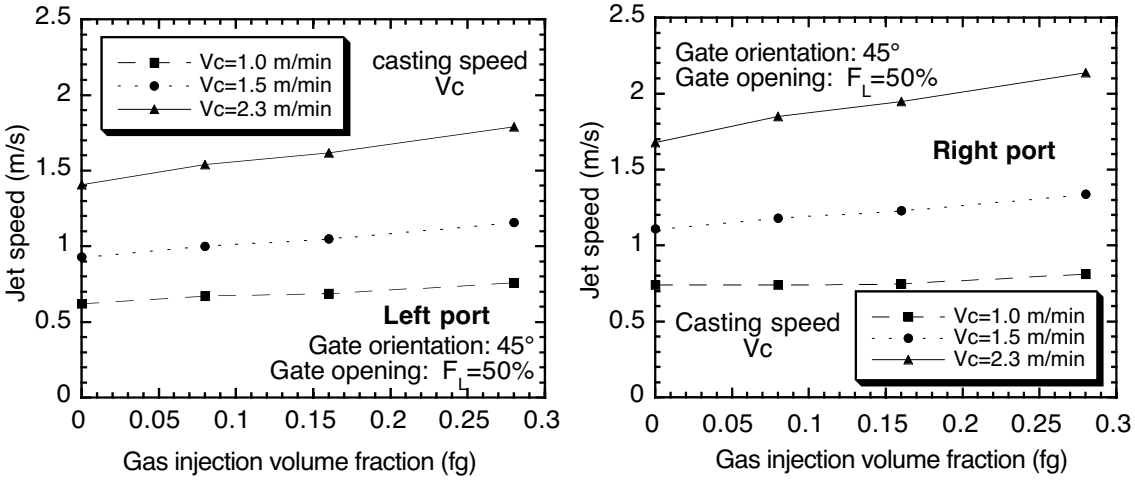

Figure 13 Effects of casting speed and gas injection on jet speed

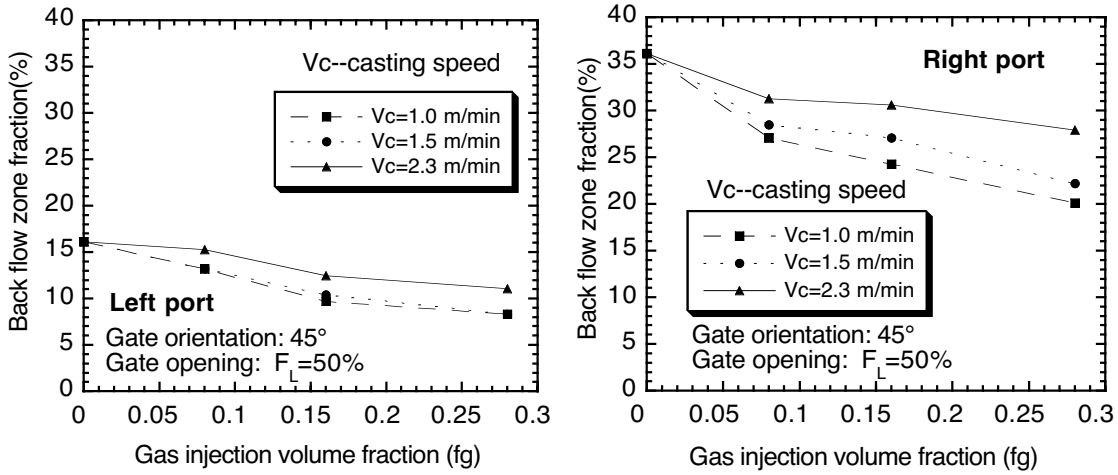

Figure 14 Effects of casting speed and gas injection on back flow zone

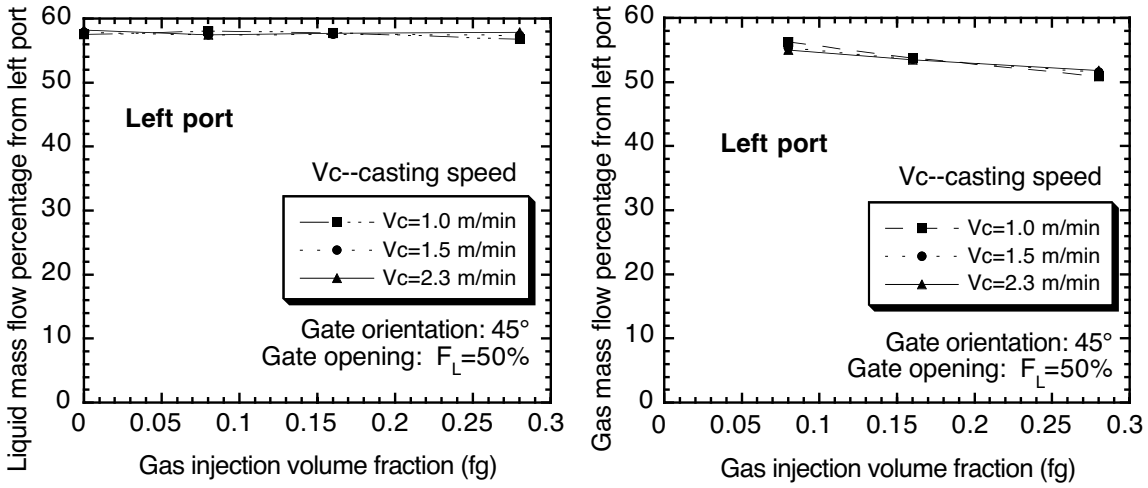

Figure 15 Effects of casting speed and gas injection on biased mass flow

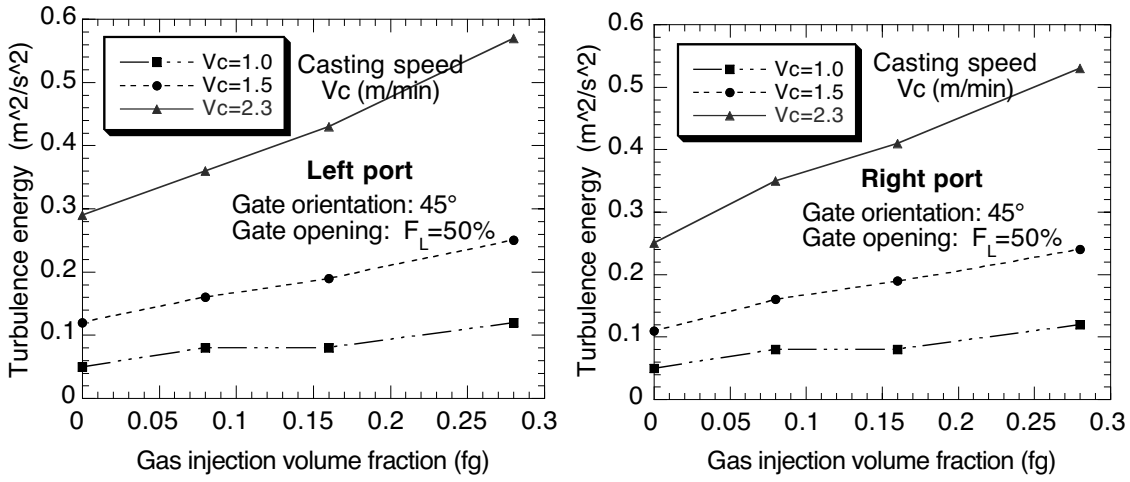

Figure 16 Effects of casting speed and gas injection on turbulence energy

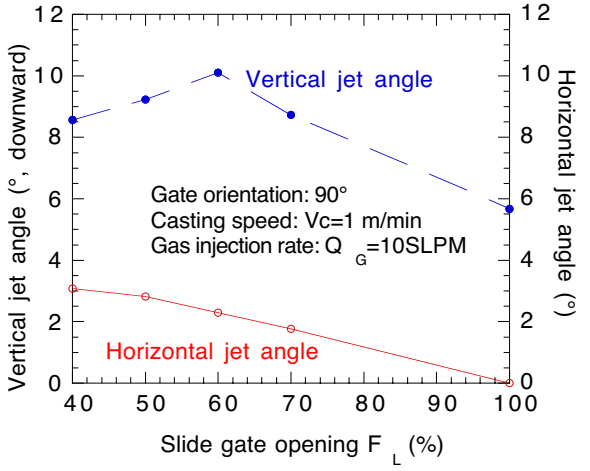

(a)

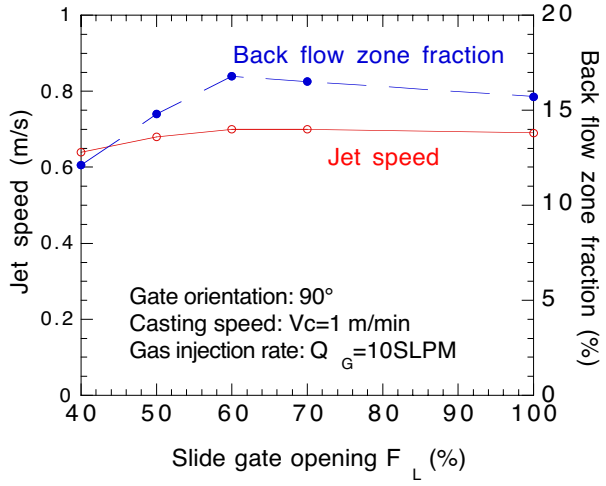

(b)

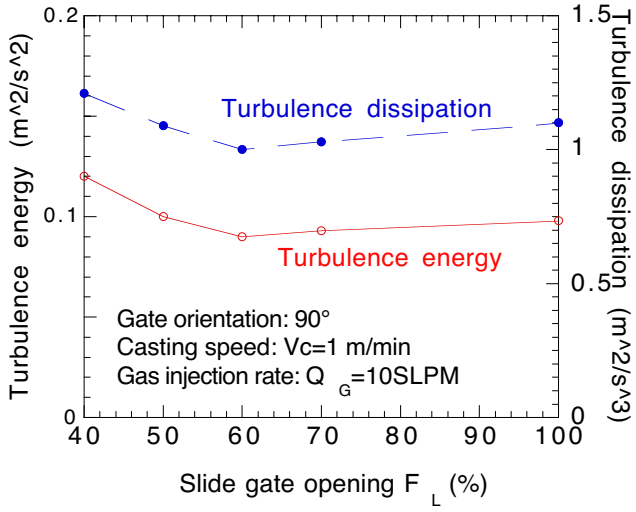

(c)

Figure 17 Effects of gate opening on (a) jet angles, (b) jet speed and back flow zone, and (c) turbulence energy and dissipation

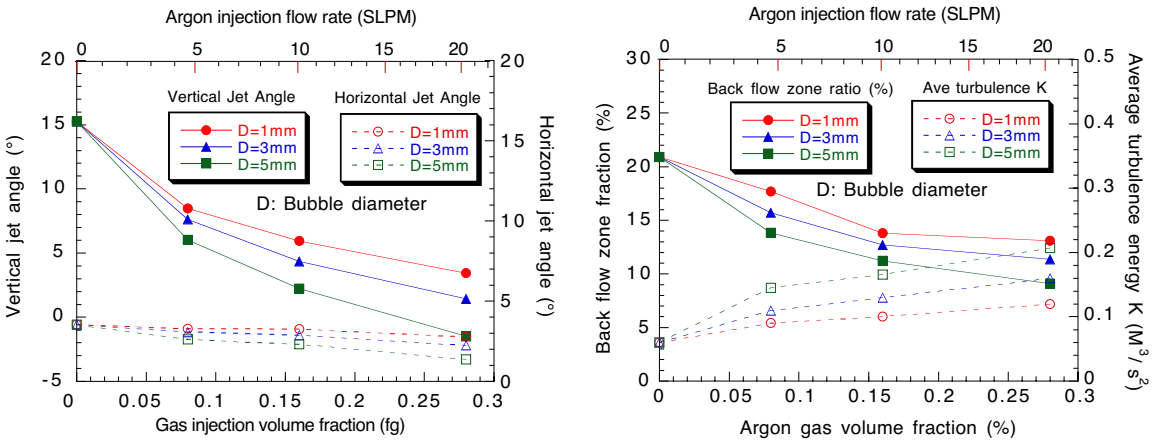

Figure 18 Effect of argon bubble size and gas injection on (a) vertical and horizontal jet angles, and (b) back flow zone and turbulence energy
(V_C=1m/min, F_L=50%, 90° orientation)

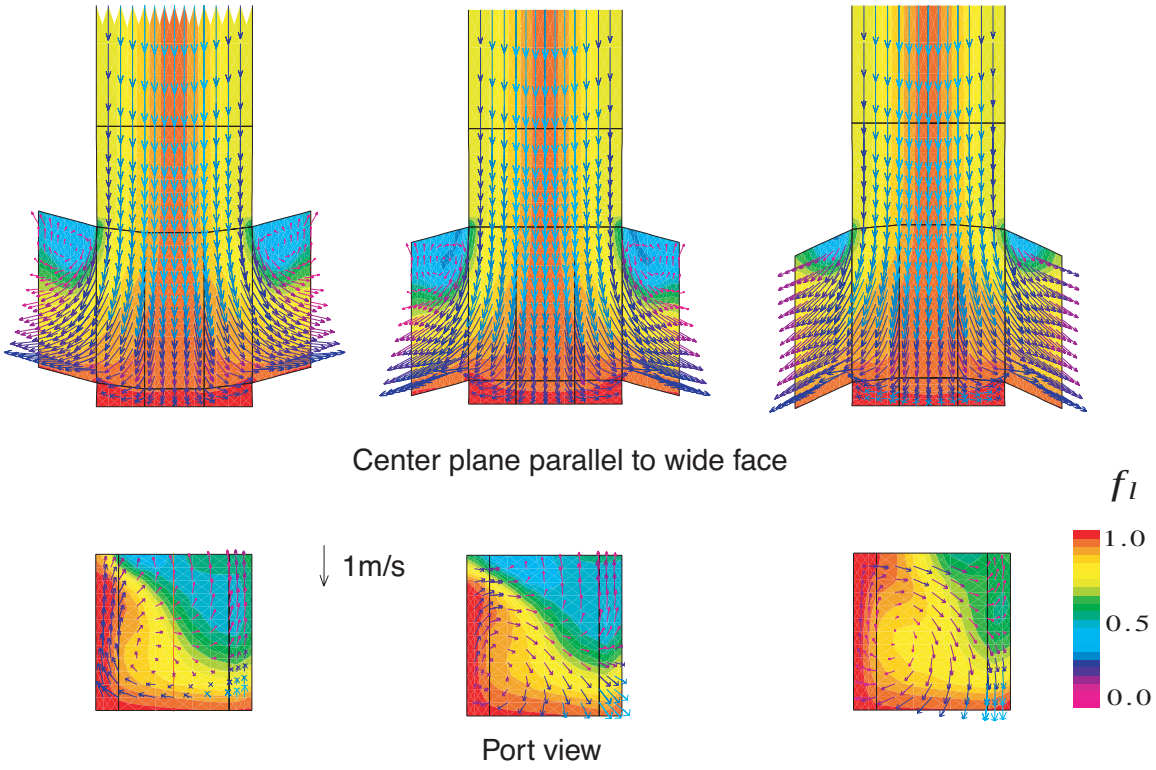

Figure 19 Liquid velocity fields superimposed on liquid volume fraction at center plane and port under different nozzle port angles (a)15° up (b) 15° down (c) 25° down (V_C=1m/min, Q_G=10SLPM, f_g=16%, F_L=50%, 90° orientation)

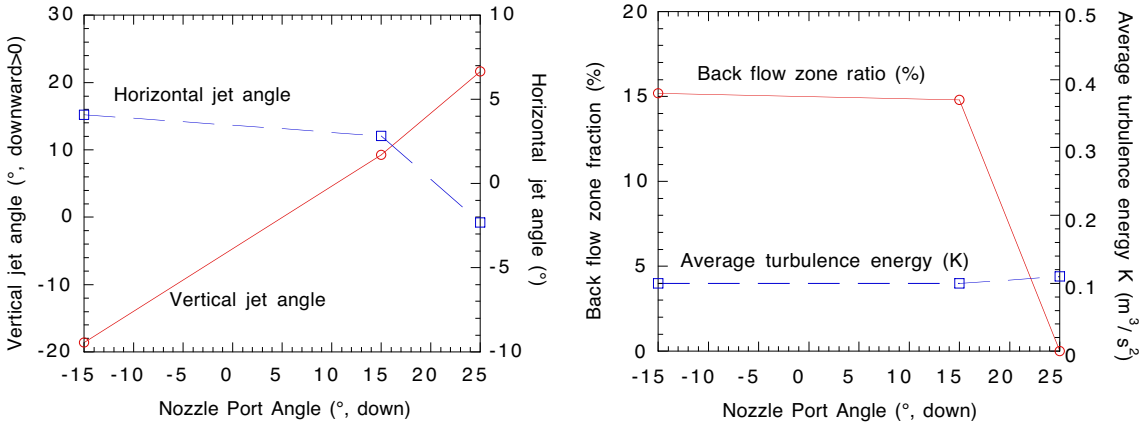

Figure 20 Effect of nozzle port angle on (a) vertical and horizontal jet angles, and (b) back flow zone and turbulence energy (V_C=1m/min, Q_G=10SLPM, f_l=16%, F_L=50%, 90° orientation)

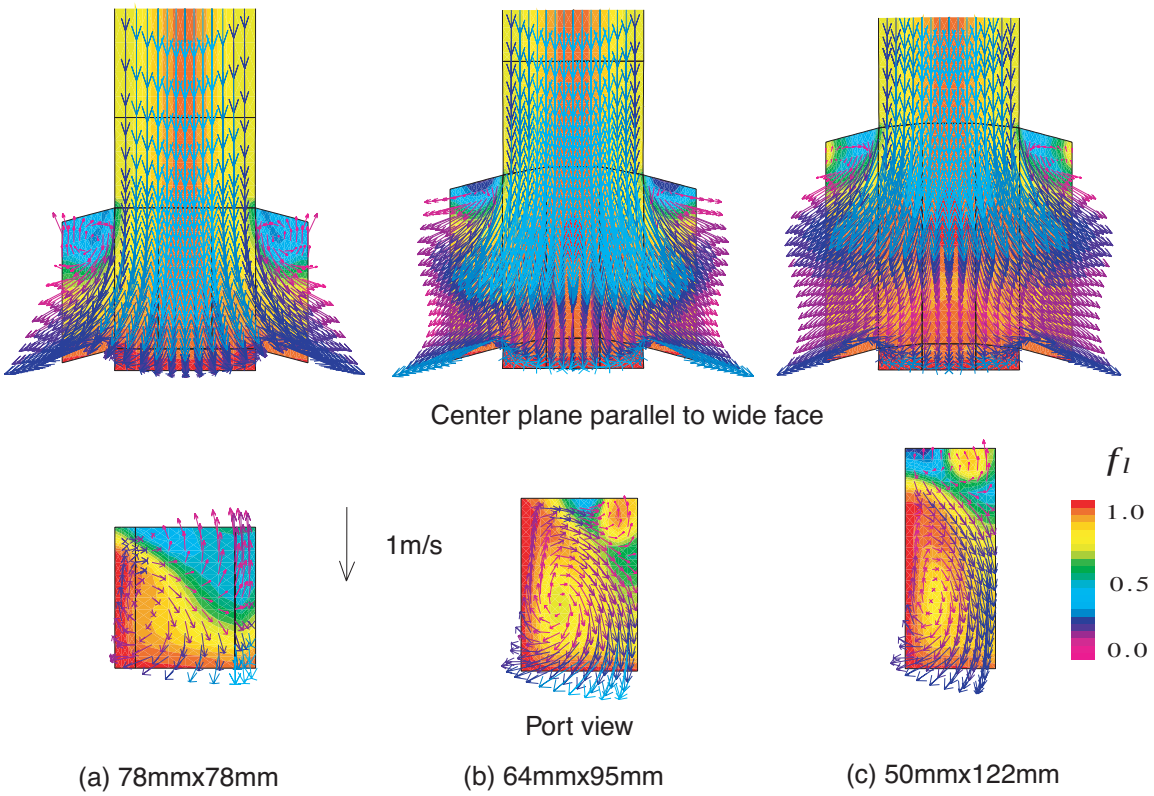

Figure 21 Liquid velocity fields superimposed on liquid volume fraction at center plane and port under different port shape designs
(V_C=1m/min, Q_G=10SLPM, f_g=16%, F_L=50%, 90° orientation)

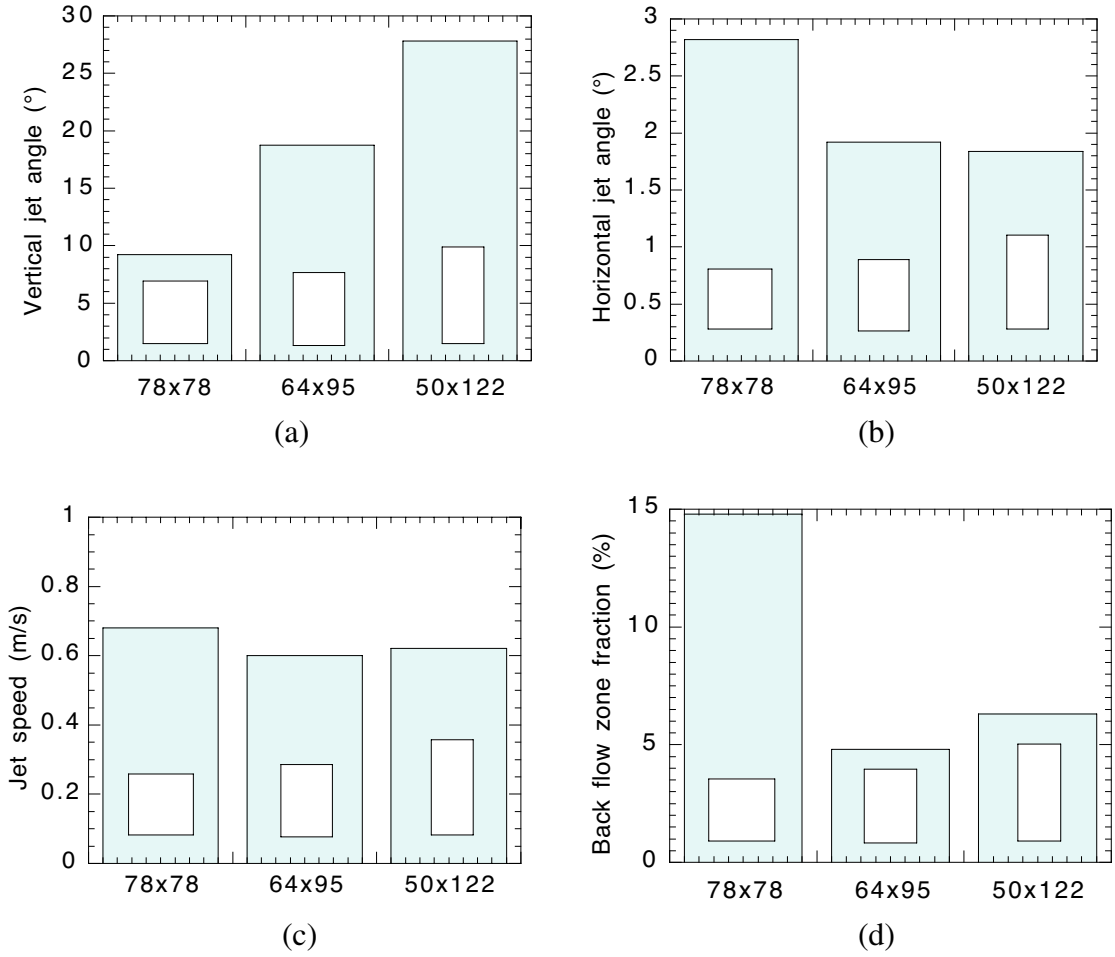

Figure 22 Effect of port shape design on (a) Vertical jet angles (b) Horizontal jet angle (c) Jet speed (d) Back flow zone ratio
(V_C=1m/min, F_L=50%, 90° orientation, 15° port angle)

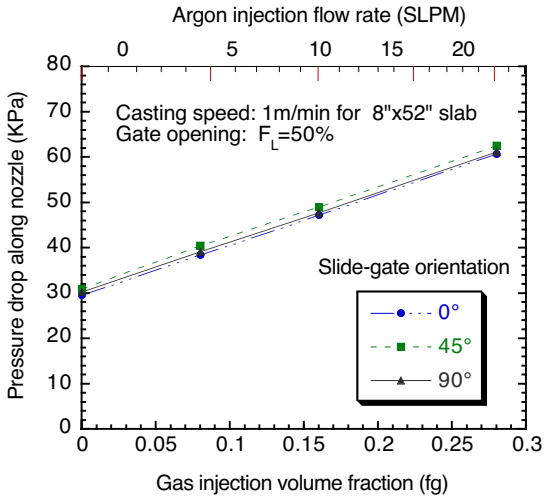

(a)

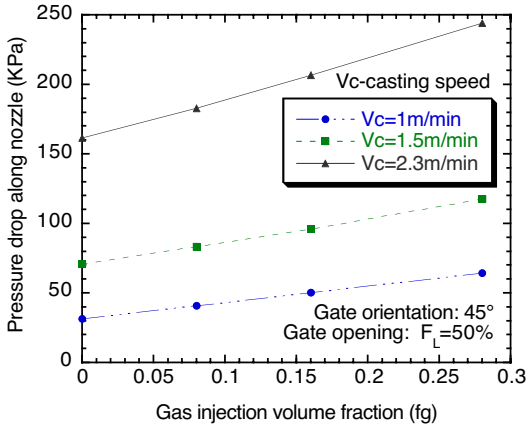

(b)

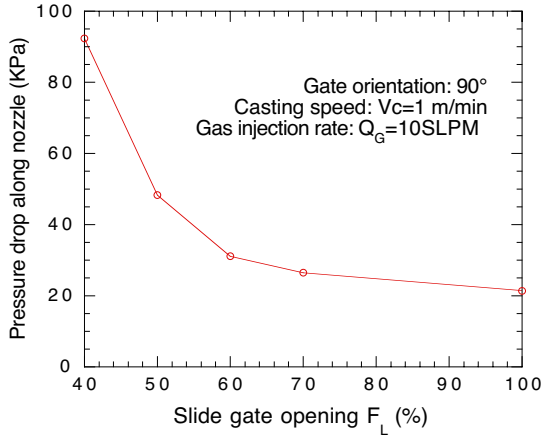

(c)

Figure 23 Effects of (a) gas injection and slide-gate orientation, (b) casting speed, and (c) slide-gate opening and on pressure drop across the nozzle